

## INSTRUMENTATION DESIGN FOR A LOW COST ELECTRICAL IMPEDANCE (EIT) SYSTEM

M. Soleimani\*, A. Movafeghi\*\* and M. H. Kargarnovin\*\*\*

\* William Lee Innovation Centre, school of materials, the University of Manchester , UK

\*\* NDT Dept., Radiation Protection Tech. Centre, AEOI, Tehran, Iran

\*\*\* School of Mechanical Engineeribg, Sharif university of Technology, Tehran, Iran

M.Soleimani-2@manchester.ac.uk , amovafeghi@gmail.com, mhkargar@sharif.edu

**Abstract:** This paper describes an impedance tomography system that can be used for the electrical conductivity imaging. Electrical Impedance Tomography provides a non-invasive method to provide useful information of tissue characteristics that cannot be obtained by other imaging modalities and requires no ionising radiation. Electrical Impedance Tomography (EIT), differentiates the differences in the electrical properties, i.e. conductivity distribution inside the object; to generate a tomographic image. Data acquisition is typically made by applying an electrical current to the object using a set of electrodes, and measuring the developed voltage between other electrodes. In practical condition EIT is very sensitive to noise. Electrodes are connected via a shielded cable to the system for noise reduction. This paper discusses an efficient and simple experimental EIT system design and the image reconstruction software developed.

### Introduction

The electrical properties of different matters have been the main topic of many investigations for many years [1,2,3]. In the Electrical Impedance Tomography (EIT), the differences in the electrical properties, i.e. conductivity distribution inside the object; is used to generate a tomographic image [2,4]. EIT is capable of handling both medicine and industrial applications [5,6,7]. The advantage of such a technique over other imaging modalities is such that, it provides a non-invasive (“non-destructive” in an industrial terminology) method and requires no ionizing radiation. Furthermore, EIT is a relative low cost and simple functional technique. Moreover, yet a portable measurement system could also be designed for it. The most important drawback of EIT is its poor image resolution, which is often restricted by the number of electrodes used for data acquisition. Data acquisition is typically made by applying an electrical current to the object using a set of electrodes, and measuring the developed voltage between other electrodes [2,8,9].

Figure 1 illustrates a general view of an EIT system. Generally 2-D the EIT systems could be categorized into two different sets namely: Applied Potential Tomography (APT) with 16 electrodes and Adaptive

Current Tomography (ACT) usually with 32 electrodes [5].

The papers should be submitted camera-ready. In the Proceedings the papers will be reproduced directly from the electronic copy submitted by the authors. The authors must strictly adhere to the instructions for preparation of camera-ready copy of their papers. Only works accepted for presentation (both oral and poster) will be published in extenso in the Conference Proceedings which will be distributed to all Conference participants at the Conference. Length of each full paper will be minimally four pages and at most six two-columns pages.

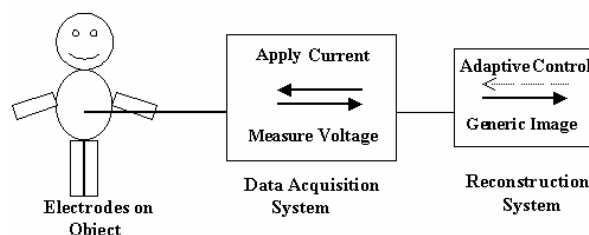


Figure 1: A general view of an EIT system.

### Materials and Methods

*Mathematical Formulations:* In a more realistic way and from a mathematical point of view; it has been shown that in the area of image reconstruction, the governing equations in the EIT field which are derivable from Maxwell’s Equations; [5] are:

$$\nabla \cdot [\tilde{\delta}(P) \cdot \nabla \tilde{U}(P)] = 0 \quad \text{at B (B is the object)} \quad (1)$$

$$\tilde{\delta}(P) \frac{\partial \tilde{U}(P)}{\partial n} = J \quad P \in S \text{ (Surface)} \quad (2)$$

$$\int_S \tilde{U}(P) ds = 0 \quad P \in S \quad (3)$$

where the  $\tilde{U}(P)$  is the voltage and  $\tilde{\delta}(P)$  is the specific admittance of B; in which:

$$\tilde{\delta}(P) = \delta(P) + j\omega\epsilon(P) \quad (4)$$

Equations (1) to (3) are the basic equations used in developing an algorithm to work in an EIT field.

In order to map the resistivity inside of a body in a more proper way, we have fabricated our own EIT system [10]. We have tested this system using both 16-electrode and 32-electrode modes of operation with different reconstruction algorithms [11]. Our prototype is an efficient and simple EIT system that is designed at Sharif University of Technology (see Figure 2). Based on this originated EIT model, a PC-base system is developed and tested with 16 and 32 electrodes in different surveys. It has to be mentioned that the system right now is only able to reconstruct the images in a 2-D domain.



Figure 2: The Overview of SUT-1 (Sharif Univ. EIT)

*EIT hardware:* The block-diagram of our EIT is shown in Figure 3. Here only the main blocks of system hardware are discussed. Moreover, for each measuring channel, a well-known block is used [3,12] (figure 4). The utilized computer is a usual Pentium-base PC, which is connected to the measurement system through an Input-Output interface (I/O) card. In the main board a current generator with 5mA @ 23 kHz and a precision voltage measurement (using synchronized pulse demodulation technique) are implemented. The accuracy of digital system is 12 bits. It is shown that the 12-bit digital resolution is a reasonable choice for the most applications [2]. The switching between different pairs of electrodes is carried out by computer using multiplexer card (MUX board). The collected data from all possible voltage measurements are fed to the image reconstruction software. In the following a brief description of any individual module of this system is shown.

*I/O card:* For I/O module, an ADVANTECH PCL-812PG I/O card is used [13]. It consists of 16 bit programmable I/O card with 12-bit successive approximation analogue to digital converter, (30 kHz sampling rate), programmable Time/Counter/Gain and two 12 bit monolithic multiplying digital to analogue converter output channels. Due to application of an unsophisticated analogue to digital conversion algorithm, it is not a fast sampling card. To overcome

this shortcoming, it is planned to use a faster card in the new version of the system.

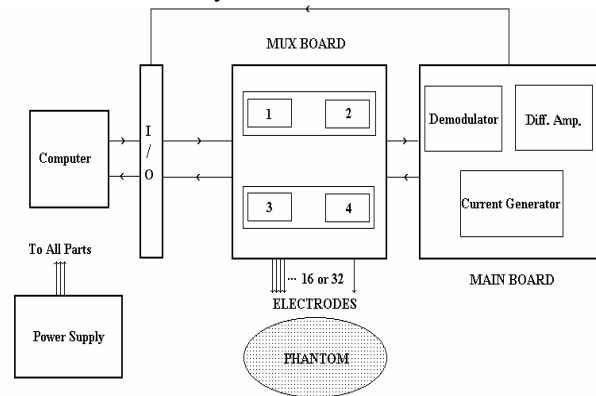


Figure 3: The block-diagram of SUT-1

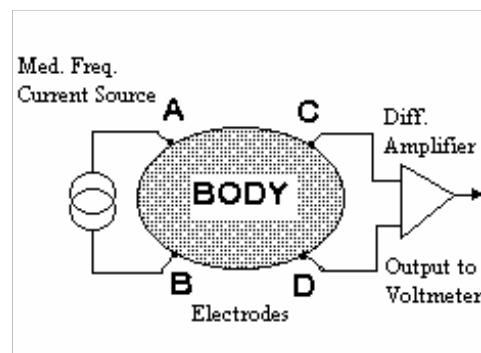


Figure 4: Each measurement channel of SUT-1

*Current Generator:* In this module we use a fixed frequency current injector. For an EIT current generator, due to its high influence in building the total system error, the amplitude stability has to be paid the highest attention on this regard [14]. Different circuits were built and tested, and finally we ended up with a digital generation method by means of an EPROM (27C258). Furthermore, the EPROM was programmed to produce 256 steps of a 23 kHz sinusoidal waveform. An 8-bit counter was used for reading of EPROM data, and then data were applied to a digital to analogue converter (DAC-0808). The system internal clock ran at 6 MHz. One of the most important advantages of this circuit is related to the synchronous pulses for demodulation, which can be obtained by the address line decoding. Zero crossing point and amplitude peak point can also be determined. The total harmonic distortion (THD) of this current generator is determined to be about 1.3%. The output of this digital oscillator is fed in to the current source through a normal gained buffer stage (LF-357). It has to be noted that our voltage control current source (VCCS) is a buffered current mirror circuit. We use Analog Devices AD-644 as the main part and some LF-411 and LF-412 for buffering. The output current could be around 5 mA.

*Voltage Measurement:* Another important part of the system hardware is the voltmeter. In EIT a synchronous differential demodulator is implemented. This method is a common method for demodulation in EIT. The noise

cancellation capability is one of the important features of this circuit. It is a “Sample and Hold” type of demodulator [15]. An AD-625 instrumentation amplifier is used as the “heart” of the measurement system. Output signal of the demodulator is fed into an I/O card by a controlled gain buffer amplifier block, which uses CA-3130 at the final stage. In APT mode of operation, the offset and gain error of this stage is of less importance, so, for a better Signal to Noise Ratio, the gain could be increased to a maximum reasonable value. The time duration in which the voltage measurement is performed, is an essential parameter in system overall speed. This time also depends on the multiplexing switching time between different channels. In order to increase the data reading time, it is possible to use, fast analogue to digital converters, separate demodulator for each channel and/or decrease in multiplexing time by means of faster digital switches. For example, in APT mode, 16 electrodes can be directly connected to our 16-bit I/O card for voltage measuring and in this way we can save multiplexing time and hence reducing errors.

We have surveyed different methods namely cross and opposite for data acquisition and their effects on distinguishability of objects [16]. An example of such methods is shown in Figure 5 in which the variations of measured voltages vs. voltage No. for a current injector are illustrated.

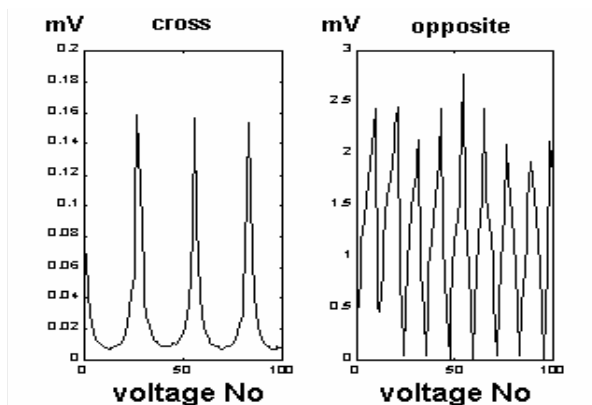


Figure 5: Variations of Measured Voltages vs. Voltage No

**Multiplexer:** In order to perform data acquisition in 32-electrodes and 16-electrodes mode, a multiplexer circuit is necessary for switching current injector and voltmeter among the different data channels. Our multiplexer circuit (MUX) consists of four 32x1 analogue multiplexers. Each multiplexer is a combination of two 16x1 IC-4067 multiplexers. The most significant type of errors arising out of MUX board, labelled as  $r_{on}$ , is related to the semiconductor switches, and also cross-talk between different channels. It has to be noted that the  $r_{on}$  does not have a constant value, but different values for different channels. It is a function of different parameters like temperature, current, etc in each channel. It is desirable to have the value of  $r_{on}$  as low as possible.

**Electrodes and Phantom:** Different cylindrical phantoms are used in this device. In order to simulate human tissues behaviour, saline solutions with different concentrations are used. Normal ECG electrodes i.e. Ag-AgCl type, is served as an electrical contacting media. Cu electrodes could be another choice for a better and more realistic simulation of electrode-skin contact impedance [17, 18].

**The software:** Here we try to overlook briefly in to the system software. According to the predefined tasks set by system hardware design, different programs were developed. In the area of data acquisition, the developed software (system control software) is written using C++ environment. In fact it can be said, this software controls the whole process. On the other hand, in the field of image reconstruction another application software is developed using MATLAB environment. Moreover, a simple program is developed which is capable of generating different meshes for Finite Element Modelling (FEM). In this F.E. model, triangular elements are used for image reconstruction (see Figure 6). Then, for the image reconstruction in the 32-electrode mode of operation, a modified Newton–Raphson method is implemented.

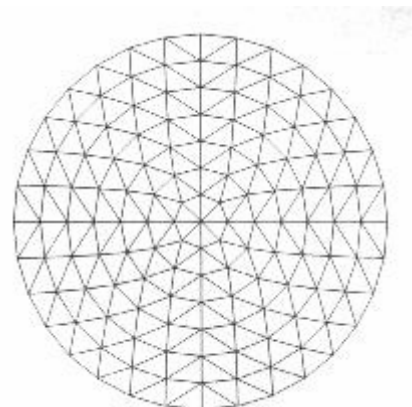


Figure 6: A Generated Mesh for Finite Element Modelling (FEM)

During APT mode of operation, image reconstruction is performed with 16 electrodes using Back Projection algorithm and iso-potential lines. Basically this was the “Sheffield Algorithm” with some changes and modifications corresponding to the specification.

## Results

The system performance was tested with different approaches i.e., the simulations and the real measurement. Here we review some examples of these results.

**Results from the simulations:** As described before, EIT is very sensitive to different errors. We tested our reconstruction software under different normal conditions and got satisfactory results by simulations.

But abnormal condition are more important regarding system overall performance. One of the interesting issues was to see what is going to happen if the positions of electrodes are changed. To do this a homogeneous medium is considered. Just one element with different resistivity was implemented at the right side of the second sector. Then 1mm error in the exact position of the electrode No.1 is introduced. The simulated data was applied to the reconstruction algorithm. The obtained result of the constructed image under this condition is shown in Figure 7. A big error is introduced specially in the adjacent elements as shown on Figure 9. The basic element is seen black (it has to be white) and this error was propagated through the image. This simulation shows mis-positioning of electrodes is one of the important issues regarding image artifacts.

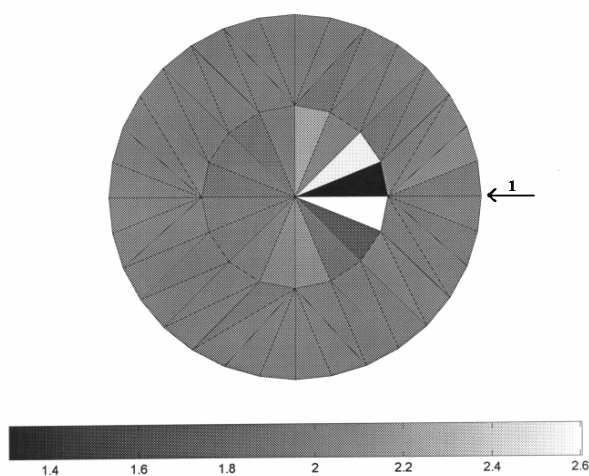


Figure 7: The error due to mis-positioning of electrodes

*Results from the real measurements:* For this part we measured the voltage and then reconstructed images in the real case both in 16 and 32 electrodes modes. In practical condition EIT is very sensitive to noise. Electrodes are connected via a shielded cable to the system for noise reduction. Figure 8 illustrates one of the actual images using a simple phantom in the APT mode. The phantom was made of PVC cylinder with 30 cm diameter and filled with saline. An object with different resistivity (a normal milk bottle) was put at the corner i.e. at  $x=6$  cm and  $y=6$  cm from geometrical center of the tank (Fig.2 shows this setup for the  $x=0$  and  $y=0$ ). Measured data were transferred to the computer, the reconstruction algorithm applied and image was obtained using back projection method. As it can be seen from Figure 10, the star artifact can be observed in the image resulted from back-projection. It is a well-known image artifact in back projection method. Basically, it is due to limitation in numbers of projection. If this projection number (ray-sum) is increased, the size this star like artifact will decrease.

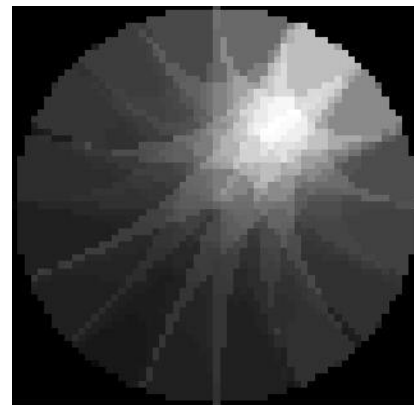


Figure 8: The Reconstructed Image with Star Artifact

### Discussion

The system is a 2-D EIT system. Its accuracy and functionality are tested at different conditions. The system is designed to be upgraded to function as a multi-current generator adaptive system. Also by modification of sampling circuit, our EIT system will be able to detect the imaginary part of the signal and accordingly phase can be detected. For this purpose voltage sampling has to be carried out during zero-crossing instead of peak sampling. The system is tested under in-vitro condition. In order to perform in-vivo measurement, the IEC-601 safety standard has to be observed. The system needs some changes using some isolation component, e.g. opto-couplers in data acquisition circuit can provide a complete electrical isolation. It is believed that the system can be also used for different EIT applications such as industrial process control.

### Conclusions

The different hardware parts of an engineered EIT system, is discussed. The system works in 2-D mode. Of course, EIT as any other device has its own limitations in practical sense. Primary studies are under way to increase its capabilities. This can be achieved by using better electrodes (e.g. active electrodes), faster data acquisition technique, multi-frequency and real time 3-D image processing. Industrial applications of system for optimizing the metallurgical and chemical processes are some other applications of this EIT system.

Results of simulation show the high capability of reconstruction software. In the real case with addition of other deteriorative parameters like noises and effects of  $r_{on}$  the system performance is affected. Especially changing in value of  $r_{on}$  makes a big error in the system performance in APT mode of operation. This effect could be decreased with direct connection and cancelling of MUX board.

## References

- [1] Grimnes S. and Martinsen O.G., (2000): 'Bioimpedance and Bioelectricity Basic', Academic Press
- [2] J. G. Webster, (1990): 'Electrical Impedance Tomography', Adam Hilger
- [3] Barber C. C. and Brown B. H., (1983): 'Imaging Spatial Distributions of Resistivity using Applied potential Tomography', *Elect. Letters*, **19**, No. 22,.
- [4] Mc Adams E. T. and Jossinet J., (1995): "Tissue impedance: a historical overview", *Physiol. Meas* **16**, pp. A1-A13
- [5] Cheney M., Isaacson D. and Newell, J. C. (1999): 'Electrical Impedance Tomography', *SIAM Review*, **41**, No. 1, pp. 85-101
- [6] Kaipio J. P. et al, (1994): 'Simulation of the Heterogeneity of Environments by Finite Element Methods', University of Kuopio, Department of Applied Physics, Finland Report No. 4/94
- [7] Mu Z. and Wexler A., (1994): 'Electrical Impedance Computed Tomography Algorithms And Application', University of Manitoba, Department of Electrical and Computer Engineering, IEEE Proc.
- [8] Savolainen T. et al, (1996): 'An EIT Measurement System for Experimental Use", University of Kuopio, Department of Applied Physics, Finland, Report No. 2/96
- [9] Savolainen T., (1999): 'Designing of a modular adaptive EIT measurement system', Department of Applied Physics, Univ. of Kuopio, Finland
- [10] Movafeghi. A., Soleimani M. et al.; (2001): 'Introducing SUT-1, A Simple and Efficient EIT System', Proc. of XI International Conference on Electrical Bio-Impedance Oslo, Norway, pp. 490-493
- [11] Movafeghi A., Nateghi A. R., M. Soleimani and Kargharnovin M. H. and Soltanian-Zadeh H., (2005): 'Image reconstruction algorithms for SUT-1 EIT system', Proc. Of XII International Conference on Electrical Bio-Impedance, Gedansk, Poland, pp. 579-582
- [12] Metherall P., (1998): '3-D EIT of the human thorax', Ph.D. thesis, University of Sheffield
- [13] User's Manual, 'PCL 812 PG, Enhanced multi-lab Card', Advantech Co. Ltd.
- [14] Blad B., Johnnesson J., Johnsson G., bachman B. and Lindsrom K., (1994): 'Waveform generator for electrical impedance tomography(EIT) using linear interpolation with multiplying D/A converters', *Journal of Medical Engineering & Technology*, **18** No.5, pp. 173-178
- [15] Koukourlis C.S., Kyriacou G.A. and Sahalos J.N, (1995): 'A 32-electrode data collection system for Electrical Impedance Tomography', *IEEE Transactions on Biomedical Engineering*, **42**, No.6, pp. 632-636
- [16] Murat Eyuboglu, B. (2000): 'Distinguishability analysis of an induced current EIT system using discrete coils', *Phy. Med. Biol.*, **45**, No. 7, pp.1997-2009
- [17] Faes T. J. et al, (1999): "The electrical resistivity of human tissue (100Hz-10MHz): a meta-analysis of review studies", *Physiol. Meas.*, **20**, pp. R1-R10
- [18] Martinsen O.G., Grimnes S. and Schwan, H.P. (2002): 'Interface Phenomena and Dielectric Properties of Biological Tissue', in 'Encyclopedia of Surface and Colloid Science', Marcel Dekker Inc. pp. 2643-2652